

# Novel hybrid of marine predator algorithm - Aquila optimizer for droop control in DC microgrid

Widi Aribowo<sup>1,2</sup>, Heri Suryoatmojo<sup>1</sup>, Feby Agung Pamuji<sup>1</sup>

<sup>1</sup>Department of Electrical Engineering, Faculty of Intelligent Electrical and Informatics Technology, Institut Teknologi Sepuluh Nopember, Surabaya, Indonesia

<sup>2</sup>Department of Electrical Engineering, Faculty of Vocational, Universitas Negeri Surabaya, Surabaya, Indonesia

## Article Info

### Article history:

Received Dec 13, 2023

Revised Feb 17, 2024

Accepted Mar 13, 2024

### Keywords:

Aquila optimizer

DC microgrid

Droop control

Load sharing

Marine predator algorithm

## ABSTRACT

This study presents a hybrid method, namely the marine predator algorithm (MPA) and Aquila optimizer (AO). The proposed algorithm is named MAO. AO duplicated the existence of the Aquila bird in nature while hunting for prey while MPA was inspired by predators in marine animal life. Although AO is widely accepted, it has several disadvantages. This causes various weaknesses such as a weak exploitation phase and slow growth of the convergence curve. Thus, certain exploitation and exploration in conventional AO can be studied to achieve the best balance. The MPA demonstrates the capacity to deliver optimal design and statistically efficient outcomes. The proposed method used AO as the main algorithm. To measure the performance of the proposed method, this study depicted a comparison using the AO, MPA, and whale optimization algorithm (WOA) methods. This paper was evaluated the performance of MAO on twenty-one CEC2017 benchmark functions test and droop control performance on direct current (DC) microgrid. From the simulation, MAO shows superior convergence ability. The proposed method and its application to droop control was successfully implemented and implied a promising performance.

*This is an open access article under the [CC BY-SA](https://creativecommons.org/licenses/by-sa/4.0/) license.*



## Corresponding Author:

Heri Suryoatmojo

Department of Electrical Engineering, Faculty of Intelligent Electrical and Informatics Technology, Institut Teknologi Sepuluh Nopember

Keputih, Sukolilo, Surabaya, East Java 60117, Indonesia

Email: suryomgt@ee.its.ac.id

## 1. INTRODUCTION

In the early 20<sup>th</sup> century, the microgrid concept was presented to combine conventional generation, distributed generation (DG) and alternating current (AC) utility lines [1]–[4]. Microgrid types are divided into two, namely AC, and DC microgrids [5]. The concept of a DC microgrid that connects power converters with renewable energy sources such as photovoltaic, wind energy sources, and energy storage systems [6]. In recent decades photovoltaic and wind energy sources have been increasingly popular in their applications. This is driven by the energy crisis and increasing environmental pollution. So the mindset of implementing green energy is getting more intense [7]. The microgrid concept has two connected modes encompassing network-connected mode, and isolated modes [8].

The AC microgrid concept is initially presented with the aim of reducing the load on the main network lines, sorting out power from renewable energy, and as a source of electrical energy in households [9]. Problems arise when the DC nature of the renewable energy source is connected to the network or converted to an AC system [10]. DC microgrid is able to increase system reliability, minimize multiple transformations, and avoid complex control of the system [11]. Problems that often occur in AC systems such

as power quality, reactive power, and frequency control can be ignored [12]. The problems that often occur in DC microgrids comprise dividing the current per unit between converters and setting the voltage at the load with a bus voltage reference [13].

In DC microgrid systems, a popular technique applied for current sharing is droop control [14]. This control can be used on both AC and DC microgrids [15]. Conventional droop control devices are applied to add virtual resistances with the aim of dividing the currents equally in DC microgrid. The problem often occurs when the bus voltage increases or decreases [16]. An approach with the conventional droop control method on DC microgrids has been widely used because it is simply applied due to the absence of a communication line. The conventional method results in inappropriate current distribution, excessive voltage fluctuation and regulation of the current circulating between the converters [17], [18]. The droop coefficient determines the accuracy of power distribution and voltage stability. More specifically, as the droop coefficient increases, the current division accuracy increases too with an intensification in the voltage variation and vice versa.

Technological developments indirectly encourage the discovery of new algorithms in optimization concepts such as metaheuristics. A remarkable improvement from the recently discovered algorithm of metaheuristics that has better performance for problem complexity. Optimization that applies traditional deterministic methods is often constrained in exploration and exploitation. Metaheuristic characteristics that are simple and easy to adjust according to the problem being addressed. Several recent metaheuristics have been presented by several researchers. A novel coati optimization algorithm (COA) is presented that emulates the natural coati's behavior. Simulating two of coati's natural behavior covers attacking and hunting iguanas, and escaping from predators which are the fundamental concept behind COA [19]. Based on Clark's nutcrackers, the nutcracker optimization algorithm (NOA) has been developed. The two different behaviors that the nutcrackers display happen at different times [20]. A copy of the red-tailed hawk is the red-tailed hawk algorithm (RTH). From the point of prey detection through the point of swoop, the red-tailed hawk has a specific hunting approach [21]. The magnifying power of an optical microscope on the target item serves as motivation for the development and application of the optical microscope algorithm (OMA) [22]. Tyrannosaurus-rex (T-Rex) optimization algorithm (TROA) is a problem-solving technique that draws inspiration from the hunting techniques of the tyrannosaurus-rex (T-Rex) dinosaur [23]. Simulating the regulations that govern the game of golf along with strategic considerations that mirror the player tactics in the game forms the conceptual basis of the golf optimization algorithm (GOA). The nuances of the GOA process are described, afterwards, there is a mathematical illustration that depicts how the two stages work together namely the exploratory phase, which is designed for global searches, and the exploitative phase, which is geared towards local searches [24].

Conventional methods of droop control result in excessive voltage changes, improper current distribution, and lack of control over the electrical current transferred between converters. The application of the metaheuristics method to droop control has been presented by several researchers and has yielded promising simulation results. Tao presents an improved fruit fly algorithm approach to be applied to droop control in inverters. The steady-state error rate is decreased by 4.3% and the inverter response speed is multiplied by 40 [25]. An improved fruit fly algorithm named the three-partition multi strategy adaptive fruit fly optimization algorithm (MSAD-FOA) is also presented by Tao and used in the inverter [26]. For frequency regulation, Rehman *et al.* [27] present an innovative master-slave droop control method. Three previous case studies also examine different effects of temperature and radiation on photovoltaic-virtual synchronous generator (PV-VSG) systems in specific locations over the course of a year. Concurrently, the ideal VSG droop control parameters are effectively optimized and frequency regulation is improved with the application of advanced particle swarm optimization (PSO) technique [27]. Improved PSO has been applied to the idea of droop control and added a fuzzy inference system (FIS) to support it [28]. The application of the PSO method is used to optimize droop reinforcement and voltage references for the purpose of minimizing channel impedance effects and can be well accommodated for marine applications [29].

During islanding, a metaheuristic technique called the salp swarm inspired algorithm (SSA) is used to regulate microgrid droop control [30]. Liang and Zou [31] introduce the Metropolis criterion of simulated annealing (SA) algorithm into the adaptive particle swarm algorithm and use a hybrid algorithm to improve droop control.

A hybrid of harmony search and genetic algorithms is applied to regulate droop control for the purpose of overcoming the reliability and technical problems of microgrids (MG) [32]. For precise division, droop parameter optimization based on the harmony search algorithm is used. Additionally, the current study uses beyond a comparative analysis of optimization performed using the harmony search method and particle swarm optimization [33]. Harris Hawks optimization (HHO) can be used in microgrid power distribution, frequency, and voltage control. According to the simulation results, the HHO droop controller enhances microgrid power quality [34]. Although several metaheuristic algorithms have been presented for optimizing

droop control, there is still much space that can be explored to obtain optimal droop control performance with different problem characteristics. Therefore, this study presents a droop control approach with the AO metaheuristic algorithm which is modified and enhanced by adding the MPA algorithm. The study contributes to several following traits: i) proposing a combination of methods namely MPA and AO named MAO, ii) conducting evaluations of the MAO's effectiveness in resolving optimization issues that have been conducted using 21 benchmarks functions, and iii) finding out the performance of the MAO method that is simulated and compared with 2 case studies, namely twenty-one CEC2017 benchmark functions test and droop control performance with comparison algorithms namely AO, MPA, and WOA. This study contains the explanation of AO, MPA, and droop control in literature review section. Section 3 shows the proposed control design and section 4 reveals a simulation result and discussion. The conclusion is disclosed in the last section.

## 2. METHOD

### 2.1. Aquila optimizer

Aquila optimizer (AO) is one of the metaheuristic algorithms introduced by Abualigah *et al.* [35]. AO is a duplicate of Aquila behavior in nature in catching prey. There are four Aquila hunting behaviors for different types of prey. Aquilas can have flexible hunting strategies for different preys. The legs and claws of the Aquilla are integrated with their speed to attack prey. The proposed AO algorithm optimization procedure is represented in four methods as follows:

Step 1: Enlarged exploration ( $X_1$ ):

At this step, Aquilla flew with a high peak in a vertical arc. Aquila behavior is represented by (1).

$$X_1(t+1) = X_{best}(t) \times \left(1 - \frac{t}{T}\right) + (X_m(t) - X_{best}(t) * rand) \quad (1)$$

$$X_M(t) = \frac{1}{N} \sum_{i=1}^N X_i(t), \forall j = 1, 2 \dots Dim \quad (2)$$

where  $X_i(t+1)$  is the completion of the next iteration  $t$ ,  $X_{best}(t)$  is the optimal solvent till the  $t^{\text{th}}$  iteration. The  $\left(1 - \frac{t}{T}\right)$  is to hold exploration.  $Dim$  is dimension value and  $N$  is the number of nominees.

Step 2: Limited exploration ( $X_2$ )

In outline flight with low glide attack. Aquila is modeled mathematically in (3).

$$X_2(t+1) = X_{best}(t) \times levy(D) + X_R(t) + (y - x) * rand \quad (3)$$

$$levy(D) = s \times \frac{u \times \sigma}{|v|^{\beta}} \quad (4)$$

$$\sigma = \left( \frac{\Gamma(1+\beta) \times \sin\left(\frac{\pi\beta}{2}\right)}{\Gamma\left(\frac{1+\beta}{2}\right) \times \beta \times 2^{\left(\frac{\beta-1}{2}\right)}} \right) \quad (5)$$

$$y = r \times \cos(\theta) \quad (6)$$

$$x = r \times \sin(\theta) \quad (7)$$

$$r = r_1 + U \times D_1 \quad (8)$$

$$\theta = -\omega \times D_1 + \theta_1 \quad (9)$$

$$\theta_1 = 3 \frac{\pi}{2} \quad (10)$$

where the solvent of the next iteration of  $t$  is  $X_2(t+1)$ ,  $levy(D)$  is the allocation aim of the fly  $levy$  and  $D$  is the dimension of solution.  $X_R(t)$  is a random completion.  $v$  is a random value.  $\beta$  is a constant value.  $y$  and  $x$  are used to represent the spiral shape in the search.  $r_1$  is a number with range 1 and 20.  $D_1$  is an integer.  $\omega$  and  $U$  are adjust to 0.005 and 0.00565.

Step 3: Enlarged exploitation ( $X_3$ )

When the prey position has been obtained, Aquila flies low by waiting for the prey's response. This step is modeled mathematically in (11).

$$X_3(t+1) = (X_{best}(t) - X_M(t)) \times \alpha - rand + ((UB - LB) \times rand + LB) \times \delta \quad (11)$$

where  $X_3(t+1)$  is the completion of the next  $t$  iteration,  $X_{best}(t)$  points to the reasonable spot of prey until the  $i^{th}$  iteration (optimal completion gained), and  $X_M(t)$  refers to mean value.  $rand$  is a random value.  $\alpha$  and  $\delta$  are the exploitation adjustment parameters set (0.1).  $LB$  and  $UB$  are the lower and upper limit.

Step 4: Limited exploitation ( $X_4$ )

In step 4, prey is hunted above the ground while Aquila runs and attacks it. The behavior of step 4 is modeled in (12).

$$X_4(t+1) = QF \times X_{best}(t) - (G_1 \times X(t) \times rand) - G_2 \times Levy(D) + rand \times G_1 \quad (12)$$

$$QF(t) = t^{\frac{2 \times rand - 1}{(t-T)^2}} \quad (13)$$

$$G_1 = 2 \times rand - 1 \quad (14)$$

$$G_2 = 2 \times (1 - \frac{t}{T}) \quad (15)$$

where  $X_4(t+1)$  is the completion of the next iteration of  $t$ .  $QF$  refers to the quality purpose applied to stability the seek strategy.

## 2.2. Marine predator algorithm

The marine predator algorithm (MPA) is one of the metaheuristic algorithms that adopts the activity of marine life between predators and prey [36]. In MPA, the position of the prey becomes a reference in updating the position. The MPA has three sessions of updating the prey's position based on speed.

Step 1: High speed

The process of finding prey is illustrated with predators and prey occupying the same area.

When  $< \frac{1}{3} \times \max\_iter$

$$\vec{Sh}_i = \vec{R}_b \otimes (\vec{Elite}_i - \vec{R}_b \otimes \vec{Prey}_i) \quad i = 1, 2, \dots, n \quad (16)$$

$$\vec{Prey}_i = \vec{Prey}_i + P \times \vec{R} \otimes \vec{Sh}_i \quad (17)$$

The  $\otimes$  is operation of multiplication.  $\vec{R}_b$  is a random value. Random numbers are based on Brownian motion.  $P$  is random value equal to 0.5.

Stage 2: Equal speed

The process of searching for prey in this phase illustrates that predators and prey are at the same speed.

When  $\frac{1}{3} \times \max\_iter < iter < \frac{2}{3} \times \max\_iter$ .

In the first population,  $\vec{R}_L$  denotes random numbers based on the distribution

$$\vec{Sh}_i = \vec{R}_L \otimes (\vec{Elite}_i - \vec{R}_L \otimes \vec{Prey}_i) \quad i = 1, 2, \dots, n/2 \quad (18)$$

$$\vec{Prey}_i = \vec{Prey}_i + P \times \vec{R} \otimes \vec{Sh}_i \quad (19)$$

In the second half of the population, the mathematical equation is drawn as (20)-(22):

$$\vec{Sh}_i = \vec{R}_b \otimes (\vec{R}_b \otimes \vec{Elite}_i - \vec{Prey}_i) \quad i = n/2, \dots, n \quad (20)$$

$$\vec{Prey}_i = \vec{Prey}_i + P \times CF \otimes \vec{Sh}_i \quad (21)$$

$$CF = (1 - \frac{iter}{\max\_iter})^{(2 \frac{iter}{\max\_iter})} \quad (22)$$

where  $CF$  serves to maintain the movement of predators adaptively

Stage 3: Low-speed

In this last phase, the prey has a speed below the predator.

When  $iter > \frac{2}{3} \times \max\_iter$

$$\vec{Sh}_i = \vec{R}_L \otimes (\vec{R}_L \otimes \vec{Elite}_i - \otimes \vec{Prey}_i) \quad i = 1 \dots n \tag{23}$$

$$\vec{Prey}_i = \vec{Prey}_i + P \times CF \otimes \vec{Sh}_i \tag{24}$$

One of the issues that sway the conduct of marine ecosystems is fish aggregating devices (FADs) which are modeled in (25).

$$\vec{Prey}_i = \begin{cases} \vec{Prey}_i + CF \times [Z_0 = Z_{min} + \vec{R} \otimes (Z_{max} - Z_{min})] \otimes A & \text{if } r \leq FADs \\ \vec{Prey}_i + [FADs (1 - r) + r](\vec{Prey}_{r1} - \vec{Prey}_{r2}) & \text{if } r > FADs \end{cases} \tag{25}$$

where  $r$  is a random value. The optimization process is affected when the  $FADs$  is 0.2.  $A$  is a binary vector.

**2.3. Droop control**

A DC microgrid system that consists of more than one source will result in a voltage difference. This will circulate current between the two DC sources. To reduce the circulating current, we can use primary control. The primary control is the initial control consisting of droop control and control loop. This is tasked with regulating the voltage and current of the system by adjusting the current that is provided to the DC bus. At this level, the load power can be shared among DC generators with communication links using distributed control techniques. Figure 1 illustrates the primary control. This control level adjusts the voltage reference provided to the internal current and voltage control loop. The output voltage can be expressed as (26):

$$V^*_o = V_{ref} - (R_d \cdot i_o) \tag{26}$$

where  $V_{ref}$  is DC bus voltage reference set point,  $R_d$  is the virtual output impedance,  $i_o$  is the output current.

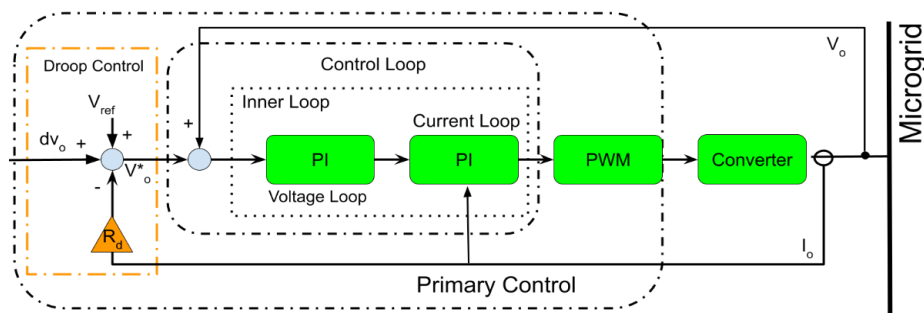


Figure 1. DC microgrid primary control

In addition to enabling the converter to operate in parallel, this control enhances the output voltage dynamic performance. Primary control enforces a performance trade-off between voltage regulation and power-sharing precision. In recent years, there has been the emergence of a variety of centralized, decentralized, and distributed techniques within hierarchical control frameworks to enhance DC microgrid reliability, adjust for voltage drift, and enhance power-sharing accuracy. Voltage drift is addressed using a secondary control. To determine the output voltage, the voltage level in the microgrid ( $V_{MG}$ ) is sensed, compared to the reference voltage  $V_{ref}$ , and the error processed through the compensator is delivered to all  $dv_o$  units as shown in Figure 2. The following is a statement of the controller:

$$dv_o = k_p (V_{ref} - V_{MG}) + k_i \int (V_{ref} - V_{MG}) dt \tag{27}$$

where  $k_p$  and  $k_i$  are the compensator secondary control control parameters. Keep in mind that  $dv_o$  needs to be constrained in order to stay under the maximum voltage deviation. Equation (27) finally becomes

$$V^*_o = V_{ref} - R_d \cdot I_o + dv_o \tag{28}$$

The source voltage, which will serve as a secondary control loop reference and can be connected to a DC source via a static bypass switch, must first be measured to connect the microgrid to a dc source.

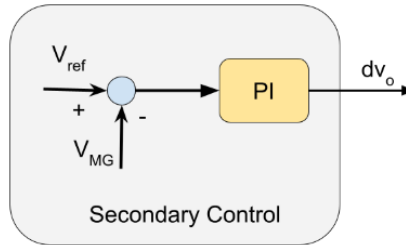


Figure 2. DC microgrid secondary control

### 3. PROPOSED MAO FOR DROOP CONTROL

The proposed method in this work combined the AO and MAO. The flowchart of the MAO method can be seen in Figure 3. The following benefits of the MAO algorithm were drawn as follow: First, by including Elite components, the exploration space was diminished. Second, by avoiding initial convergence, the MAO algorithm had attractive research and exploitation domains. The suggested approach included a top predator. In nature, top predators were better at finding food. As a result, the strongest solution was chosen as the top predator to create the Elite matrix, which can be modeled as (29):

$$Elite = \begin{bmatrix} A^I_{1.1} & A^I_{1.2} & \dots & A^I_{1.d} \\ A^I_{2.1} & A^I_{2.2} & \dots & A^I_{2.d} \\ \vdots & \vdots & \vdots & \vdots \\ A^I_{n.1} & A^I_{n.2} & \dots & A^I_{n.d} \end{bmatrix} \tag{29}$$

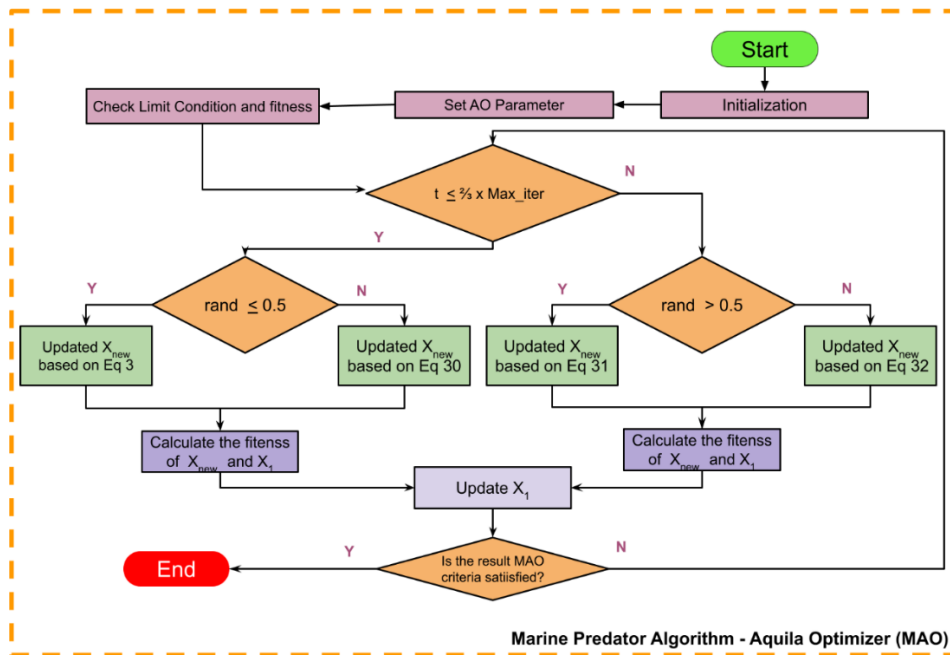


Figure 3. The flowchart of MAO

The steps of the proposed method are as follows:

- Add to (3) with (16) so it becomes the (30):

$$\vec{Sh}_i = X_2 \times \vec{R}_b \otimes (\vec{Elite}_i - \vec{R}_b \times X_2(t)) \quad (30)$$

- Replace (11) with (18) so it becomes (31):

$$X_3(t+1) = \vec{R}_L \otimes (\vec{Elite}_i - \vec{R}_L \times X_3(t)) \quad (31)$$

- Modify (12) by adding (23) so it becomes (32).

$$X_4(t+1) = QF \times \vec{R}_L \otimes (\vec{R}_L \otimes \vec{Elite}_i - X_4(t)) \times G_1 \quad (32)$$

## 4. RESULTS AND DISCUSSION

### 4.1. Convergence curve profile

The benchmark function was used to assess MAO performance. Consideration of 21 literary mathematical functions was the initial stage. The mathematical function consisted of 8 fixed-dimensional multimodal functions F14-F21, 6 multimodal functions F8-F13, and 7 unimodal functions F1-F7. MATLAB Simulink software was used to execute the simulation, and a laptop with an Intel I5-5200 2.19 GHz processor and 8 GB RAM was employed. Table 1 shows a list of the MAO parameters used in the simulation.

The three categories benchmark function had their own characteristics. The unimodal function had one global ideal and no local optimal, making it a good candidate for benchmarking algorithm exploitation. The multimodal function was particularly useful for assessing exploration and deducting the algorithm local optima position since it had many local optimum points.

Performance evaluation of the MAO used the AO, WOA, and MPA approaches. Convergence graph performance assessment was measured based on the lowest value obtained. Figure 4 show that the MAO algorithm performed all algorithms on 21 functions. While the lowest convergence value for F8 was the WOA algorithm. In the F14, F15, F17, F19 and F20 function, the lowest convergence value was MPA. In function 21, MAO and AO had similar and lowest convergence curves. MAO had the lowest convergence curve in the functions F1, F1, F3, F4, F5, F6, F7, F9, F10, F11, F12 and F13.

Table 1. Parameter of MAO

No.	Parameter	Value
1	Alpha ( $\alpha$ )	0.1
2	Delta ( $\delta$ )	0.1
3	Omega ( $\omega$ )	0.005
4	Beta ( $\beta$ )	1.5
5	$r_1$	10
6	$U$	0.00565

### 4.2. Utilizing MAO to control droop

The DC microgrid configuration consisted of two sources encompassing a PV and a DC generator (DCG), which were both connected to a DC load. a 100 V DC bus voltage low voltage DC microgrid. In addition to supplying DC loads, this low voltage was frequently employed in residential setups. Table 2 shows the details of the system used. A representation of a DC microgrid block as shown in Figure 5.

Regarding Figure 5, the difference between the reference voltage and the bus voltage produced an error. After taking the absolute value multiplied by time it was then converted to ITAE. ITAE results were used to repeat the iteration of MAO. The results of the MAO iteration were the parameters of the proportional-integral (PI) in the voltage loop, PI in the current loop, PI in the secondary control and the value of the droop coefficient in each converter. This was because ITAE, in contrast to its rival's integral absolute error (IAE), integral square error (ISE), and integral time squared error (ITSE), allowed for smoother implementation and produced superior results. The harsh criteria ITSE and ISE produced unrealistic evaluations because they squared errors. IAE was also an inadequate option compared to ITAE which represented a more realistic error index due to the time multiplier error function. Therefore, ITAE was used for optimization in this study. The mathematical definition of ITAE can be drawn as follows:

$$ITAE = \int_0^{\infty} t \cdot e(t) \cdot dt \quad (33)$$

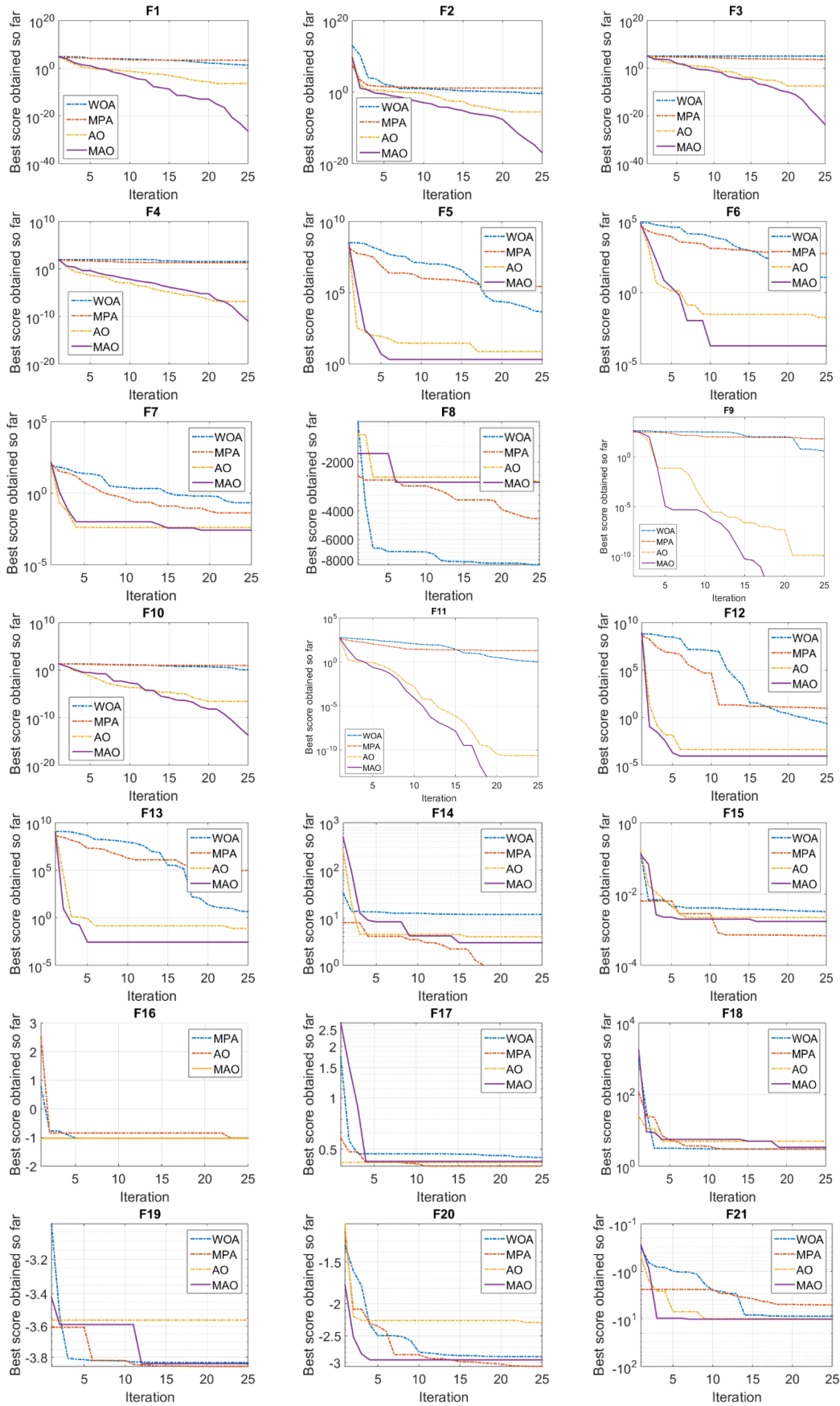


Figure 4. Convergence curves of algorithms on respective benchmark test



Table 2. System parameter

No.	Simulation parameters Parameter	Value
1	Voltage bus	100 V
2	Capacitance of converter	40,000 $\mu$ F
3	Inductance of converter	2e-3 mH
4	Switching frequency of converter	10 kHz
5	Line resistance for PVG	0.22 $\Omega$
6	Line resistance for DCG	0.018 $\Omega$

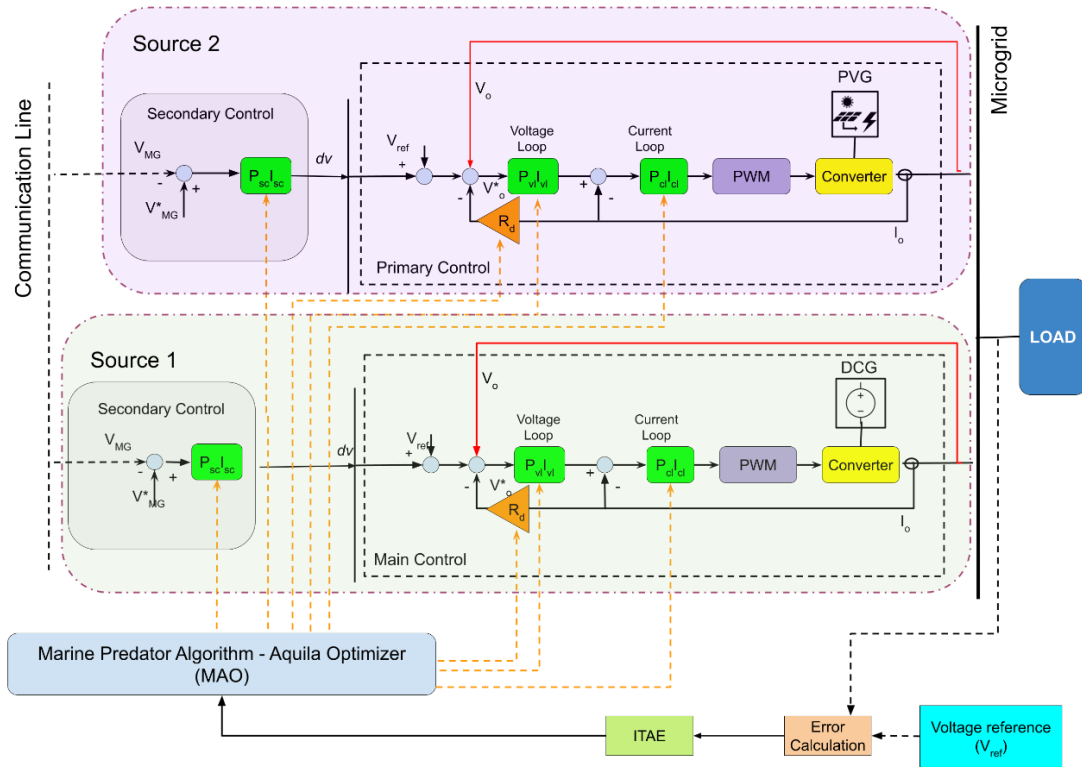


Figure 5. Block representation of the islanded DCMG

To evaluate the proposed control strategy performance. Simulink was used to model and simulate the system in accordance with the fundamental ideas of section 2, with the dc bus voltage set to 100 V. Tables 3 and 4 show the optimization results with each method used in this study. It was significant to note that the overshooting/undershooting levels of microgrid voltage, power sharing, and system responsiveness had been used to evaluate the durability of the suggested technique.

Table 3. The value of PI control for each algorithm in source 1

Methods	$P_{vl}$	$I_{vl}$	$P_{cl}$	$I_{cl}$	$P_{sc}$	$I_{sc}$	$R_d$
WOA	0.2470	0.4196	0.8279	0.2785	0.7103	0.6966	0.5311
MPA	0.7885	0.6437	0.7857	0.444	0.8594	0.8541	0.7158
AO	0.2797	0.673	0.1670	0.3614	0.7801	0.8385	0.1678
MAO	0.9638	0.722	0.0948	0.7736	0.5277	0.2355	0.4578

Table 4. The value of PI control for each algorithm in source 2

Methods	$P_{vl}$	$I_{vl}$	$P_{cl}$	$I_{cl}$	$P_{sc}$	$I_{sc}$	$R_d$
WOA	0.4818	0.0073	0.4947	0.2645	0.5102	0.0956	0.3976
MPA	0.189	0.3571	0.1003	0.2978	0.7689	0.8487	0.775
AO	0.5819	0.5271	0.3857	0.3008	0.578	17.9282	25.9
MAO	0.9572	0.0048	0.2166	0.7092	0.2289	0.2808	0.2751

The system was loaded by 4.2 ohms between seconds 0 and 2. Table 5 shows the details of the system response from each method. Figure of voltage and power responses were presented in Figures 6(a) and 6(b). At voltage, the ITAE value was 0.3714 and an overshoot of 0.1413 V was obtained from the MAO method. The ITAE value of the MAO method was better than the AO method, which was 0.353% and the MPA method, which was 24.03%.

The distribution of current to the load between the two sources is illustrated in Figure 7. Sources 1 and 2 from each algorithm provide different responses. In Figures 6(a) and 6(b), the comparison of the response given by voltage and power to changes in load in each algorithm is very slight. The comparison of currents that experience changes in load forms a different character for each algorithm. In Figure 7(a) the WOA algorithm response has an overshoot of 18.93A. The AO algorithm response to changes in load has an overshoot of 13.4A which can be seen in Figure 7(b). Figures 7(c) and 7(d) are the algorithm responses from the MPA and MAO methods which have overshoots of 15.03A and 11.93A.

Table 5. Transient response of voltage

Methods	Overshoot	Undershoot	ITAE
WOA	0.1500	No Undershoot	0.3728
AO	0.1418	No Undershoot	0.3737
MPA	0.1860	No Undershoot	0.3729
MAO	0.1413	No Undershoot	0.3714

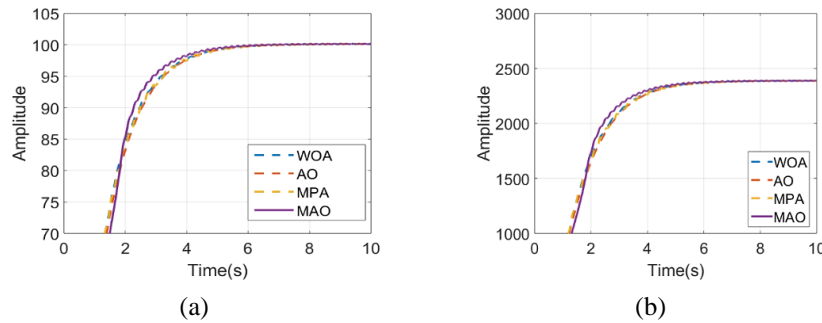


Figure 6. Illustration of a transient (a) response of voltage and (b) response of power

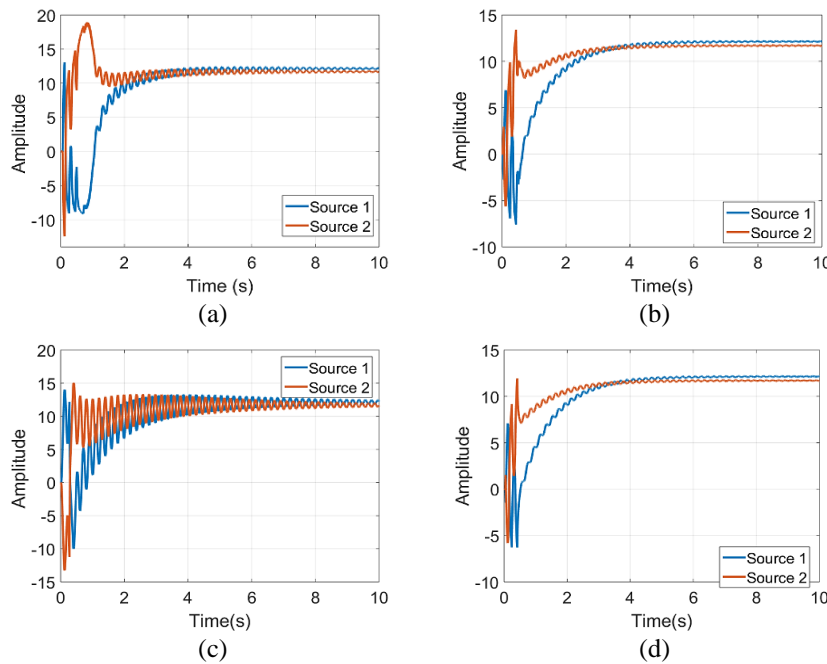


Figure 7. Response of current (a) WOA (b) AO (c) MPA (d) MAO

It can be seen in Table 6 that the difference in current values between the two sources which has the smallest difference is the MAO method of 0.4433. Meanwhile, the current value from the source that has the largest value is MPA of 0.4788. The lowest overshoot value in Table 6 is MAO of 11.93. Meanwhile, the highest is WOA of 18.93. The overshoot value of MAO is better at 7% than WOA, 1.47% than AO and 3.1% than MPA.

The next test of the MAO method is to change the load. For the first time, the system is loaded at 4.2 ohms from seconds 0 to 2. The load was increased by 10 ohms from the 2nd second and continued until 4<sup>th</sup> seconds. 8.6 ohms was added to the load once more at 4th second. At 6th seconds, the load was decreased by 6 ohms. Figure 8 is an illustration of load changes that occur on the system. An illustration of changes in load to system power can be seen in Figure 8(a). At 0 to 2 seconds, the voltage value is 100.1 V. The load increases by 10 ohms in the 2<sup>nd</sup> second. The steady state voltage value is 99.92 V from 2<sup>nd</sup> to 4<sup>th</sup> seconds. In the 4<sup>th</sup> second, the load value increases by 8.6 ohms. The steady state voltage value is 99.67 V. At the 6<sup>th</sup> second, the load value drops by 6 ohms. The steady state voltage value is 100 V. An illustration of load changes that affect voltage and current can be seen in Figure 8(b) and Figure 8(c).

Table 6. The result of current

Methods	Overshoot	Undershoot	Error
WOA	18.93	-12.32	0.4527
AO	13.4	-7.598	0.4452
MPA	15.03	-13.25	0.4788
MAO	11.93	-6.298	0.4433

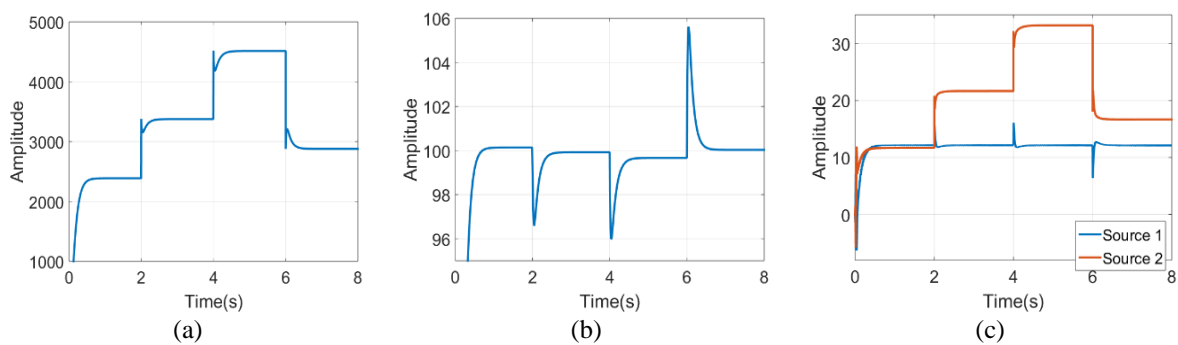


Figure 8. Illustration of load changes (a) response of power, (b) response of voltage, and (c) response of current

## 5. CONCLUSION

The Aquila optimizer is characterized by four distinct methods. These methods include selecting the search space through high soaring with vertical stoop, exploring within a divergent search space through contour flight with short glide attack, exploiting within a convergent search space through low flight with slow descent attack, and finally swooping by walking and grabbing prey. The MPA refers to the often-observed foraging behavior shown by ocean predators, characterized by a combination of Lévy and Brownian motions. This strategy is accompanied by an optimal encounter rate policy, which governs the biological interaction between predator and prey. This study proposes a hybrid method, namely aquila optimizer and marine predator algorithm called MAO. This study uses CEC2017 benchmark functions comparisons and droop control on the DC microgrid system to determine performance. AO, MPA, and WOA methods are also employed in the present study. From the CEC2017 benchmark function comparison, the MAO method has the lowest convergence curve of 12 compared to the other methods. From the simulation on droop control, it is revealed that the MAO method is a better ITAE than, namely 0.4022% compared to MPA, 0.3755% compared to WOA, and 0.6155% compared to AO. The control provides a reliable response when load changes occur. Based on the results, it was found that the highest voltage drop was 0.38%. Therefore, the MAO method has an effective and promising performance. AO and MPA are combined in the MAO technique. Reviewing applications for complicated and binary systems is necessary to achieve better exploration and exploitation performance outcomes. Aside from that, further study is required on droop control, including the use of the most recent control techniques.




## REFERENCES

- [1] A. Raza, Q. Huang, J. Li, O. Bamisile, M. Afzal, and G. Raza, "Adaptive drooping control scheme for VSC-MTDC system with multiple renewable energy sites based on variable droop constant," *International Journal of Electrical Power & Energy Systems*, vol. 144, Jan. 2023, doi: 10.1016/j.ijepes.2022.108520.
- [2] S. Alghamdi *et al.*, "Reduction in voltage harmonics of parallel inverters based on robust droop controller in islanded microgrid," *Mathematics*, vol. 11, no. 1, Dec. 2022, doi: 10.3390/math11010172.
- [3] T. Lan and K. Strunz, "Droop control for district heating networks: solution for temperature control of multi-energy system with renewable power supply," *International Journal of Electrical Power & Energy Systems*, vol. 146, Mar. 2023, doi: 10.1016/j.ijepes.2022.108663.
- [4] Y. Mi, J. Deng, X. Yang, Y. Zhao, S. Tian, and Y. Fu, "The novel multiagent distributed SOC balancing strategy for energy storage system in DC microgrid without droop control," *International Journal of Electrical Power & Energy Systems*, vol. 146, Mar. 2023, doi: 10.1016/j.ijepes.2022.108716.
- [5] S. Liu, H. Miao, J. Li, and L. Yang, "Voltage control and power sharing in DC Microgrids based on voltage-shifting and droop slope-adjusting strategy," *Electric Power Systems Research*, vol. 214, Jan. 2023, doi: 10.1016/j.epr.2022.108814.
- [6] C. Xiang, Q. Cheng, Y. Zhu, and H. Zhao, "Sliding mode control of ship DC microgrid based on an improved reaching law," *Energies*, vol. 16, no. 3, Jan. 2023, doi: 10.3390/en16031051.
- [7] M. S. Alam, F. S. Al-Ismail, F. A. Al-Sulaiman, and M. A. Abido, "Energy management in DC microgrid with an efficient voltage compensation mechanism," *Electric Power Systems Research*, vol. 214, Jan. 2023, doi: 10.1016/j.epr.2022.108842.
- [8] W. Aribowo, H. Suryatomo, and F. A. Pamuji, "Optimization droop control based on Aquila optimizer algorithm for DC microgrid," in *2022 International Seminar on Intelligent Technology and Its Applications (ISITIA)*, Jul. 2022, pp. 460–465, doi: 10.1109/ISITIA56226.2022.9855330.
- [9] M. Hajhosseini, V. Lešić, H. I. Shaheen, and P. Karimaghaee, "Sliding mode controller for parameter-variable load sharing in islanded AC microgrid," *Energies*, vol. 15, no. 16, Aug. 2022, doi: 10.3390/en15166029.
- [10] N. Zhang, D. Yang, H. Zhang, and Y. Luo, "Distributed control strategy of DC microgrid based on consistency theory," *Energy Reports*, vol. 8, pp. 739–750, Nov. 2022, doi: 10.1016/j.egy.2022.05.189.
- [11] R. Dadi, K. Meenakshy, and S. K. Damodaran, "A review on secondary control methods in DC microgrid," *Journal of Operation and Automation in Power Engineering*, vol. 11, no. 2, pp. 105–112, 2023.
- [12] X. Jin, Y. Shen, and Q. Zhou, "A systematic review of robust control strategies in DC microgrids," *The Electricity Journal*, vol. 35, no. 5, Jun. 2022, doi: 10.1016/j.tej.2022.107125.
- [13] V.-V. Thanh and W. Su, "Improving current sharing and voltage regulation for DC microgrids: a decentralized demand response approach," *IEEE Transactions on Smart Grid*, vol. 14, no. 4, pp. 2508–2520, Jul. 2023, doi: 10.1109/TSG.2022.3222220.
- [14] A. Aluko, A. Swanson, L. Jarvis, and D. Dorrell, "Modeling and stability analysis of distributed secondary control scheme for stand-alone DC microgrid applications," *Energies*, vol. 15, no. 15, Jul. 2022, doi: 10.3390/en15155411.
- [15] C. Gomez-Aleixandre, A. Navarro-Rodriguez, G. Villa, C. Blanco, and P. Garcia, "Adaptive droop controller for a hybrid 375 Vdc/48 Vdc/400 Vac AC/DC microgrid," *IEEE Transactions on Industry Applications*, vol. 58, no. 4, pp. 5104–5116, Jul. 2022, doi: 10.1109/TIA.2022.3176597.
- [16] A. F. Habibullah and K.-H. Kim, "Decentralized power management of DC microgrid based on adaptive droop control with constant voltage regulation," *IEEE Access*, vol. 10, pp. 129490–129504, 2022, doi: 10.1109/ACCESS.2022.3228703.
- [17] R. Kumar and M. K. Pathak, "Distributed droop control of dc microgrid for improved voltage regulation and current sharing," *IET Renewable Power Generation*, vol. 14, no. 13, pp. 2499–2506, Oct. 2020, doi: 10.1049/iet-rpg.2019.0983.
- [18] W. Aribowo, "Slime mould algorithm training neural network in automatic voltage regulator," *Trends in Sciences*, vol. 19, no. 3, pp. 1–11, 2022, doi: 10.48048/tis.2022.2145.
- [19] M. Dehghani, Z. Montazeri, E. Trojovská, and P. Trojovský, "Coati optimization algorithm: a new bio-inspired metaheuristic algorithm for solving optimization problems," *Knowledge-Based Systems*, vol. 259, Jan. 2023, doi: 10.1016/j.knosys.2022.110011.
- [20] M. Abdel-Basset, R. Mohamed, M. Jameel, and M. Abouhawwash, "Nutcracker optimizer: a novel nature-inspired metaheuristic algorithm for global optimization and engineering design problems," *Knowledge-Based Systems*, vol. 262, Feb. 2023, doi: 10.1016/j.knosys.2022.110248.
- [21] S. Ferahtia *et al.*, "Red-tailed hawk algorithm for numerical optimization and real-world problems," *Scientific Reports*, vol. 13, no. 1, p. 12950, 2023.
- [22] M.-Y. Cheng and M. N. Sholeh, "Optical microscope algorithm: a new metaheuristic inspired by microscope magnification for solving engineering optimization problems," *Knowledge-Based Systems*, vol. 279, Nov. 2023, doi: 10.1016/j.knosys.2023.110939.
- [23] V. S. D. M. Sahu, P. Samal, and C. K. Panigrahi, "Tyrannosaurus optimization algorithm: a new nature-inspired meta-heuristic algorithm for solving optimal control problems," *e-Prime - Advances in Electrical Engineering, Electronics and Energy*, vol. 5, Sep. 2023, doi: 10.1016/j.prime.2023.100243.
- [24] Z. Montazeri, T. Niknam, J. Aghaei, O. P. Malik, M. Dehghani, and G. Dhiman, "Golf optimization algorithm: a new game-based metaheuristic algorithm and its application to energy commitment problem considering resilience," *Biomimetics*, vol. 8, no. 5, Aug. 2023, doi: 10.3390/biomimetics8050386.
- [25] X. Tao, L. Zhang, and F. Wang, "Droop control optimization strategy for parallel inverters in a microgrid based on an improved population division fruit fly algorithm," *IEEE Access*, vol. 10, pp. 24877–24894, 2022, doi: 10.1109/ACCESS.2022.3145965.
- [26] X. Tao, L. Zhang, F. Wang, G. Tian, and H. Zhang, "Three-partition multistrategy adaptive fruit fly optimization algorithm for microgrid droop control," *International Transactions on Electrical Energy Systems*, vol. 2022, pp. 1–20, Jan. 2022, doi: 10.1155/2022/2646384.
- [27] H. U. Rehman *et al.*, "Droop control design based on advanced particle swarm optimization for grid-connected multi PV-VSG," in *The 16th IET International Conference on AC and DC Power Transmission (ACDC 2020)*, 2021, pp. 2214–2220, doi: 10.1049/icp.2020.0332.
- [28] L. Zhang, H. Zheng, Q. Hu, B. Su, and L. Lyu, "An adaptive droop control strategy for islanded microgrid based on improved particle swarm optimization," *IEEE Access*, vol. 8, pp. 3579–3593, 2020, doi: 10.1109/ACCESS.2019.2960871.
- [29] R. Dahiya, "Voltage regulation and enhance load sharing in DC microgrid based on particle swarm optimization in marine applications," 2017.
- [30] M. A. Ebrahim, R. M. A. Fattah, E. M. Saied, S. M. A. Maksoud, and H. El Khashab, "Salp swarm optimization with self-adaptive mechanism for optimal droop control design," in *Electric Power Conversion and Micro-Grids*, IntechOpen, 2022.
- [31] J. Liang and H. Zou, "Microgrid droop control based on simulated annealing adaptive particle swarm optimization," *Journal of Physics: Conference Series*, vol. 2355, no. 1, Oct. 2022, doi: 10.1088/1742-6596/2355/1/012052.




- [32] M. Abedini, M. H. Moradi, and S. M. Hosseini, "Optimal clustering of MGs based on droop controller for improving reliability using a hybrid of harmony search and genetic algorithms," *ISA transactions*, vol. 61, pp. 119–128, 2016.
- [33] P. Monica and M. Kowsalya, "Improved harmony search based optimization of droop control parameters for load sharing in DC microgrids," in *TENCON 2019-2019 IEEE Region 10 Conference (TENCON)*, 2019, pp. 2199–2203.
- [34] M. A. Ebrahim, R. M. A. Fattah, E. M. Saied, S. M. A. Maksoud, and H. El Khashab, "Droop control of an islanded microgrid using Harris Hawks optimization algorithm," *International Journal of Applied Mathematics, Computational Science and Systems Engineering*, vol. 3, 2021.
- [35] L. Abualigah, D. Yousri, M. Abd Elaziz, A. A. Ewees, M. A. A. Al-qaness, and A. H. Gandomi, "Aquila optimizer: A novel meta-heuristic optimization algorithm," *Computers & Industrial Engineering*, vol. 157, Art. no. 107250, Jul. 2021, doi: 10.1016/j.cie.2021.107250.
- [36] A. Faramarzi, M. Heidarinejad, S. Mirjalili, and A. H. Gandomi, "Marine predators algorithm: a nature-inspired metaheuristic," *Expert Systems with Applications*, vol. 152, Aug. 2020, doi: 10.1016/j.eswa.2020.113377.

## BIOGRAPHIES OF AUTHORS






**Widi Aribowo**    is a lecturer in the Department of Electrical Engineering, Universitas Negeri Surabaya, Indonesia. He is B.Sc. in power engineering at Sepuluh Nopember Institute of Technology (ITS), Surabaya in 2005. He is M.Eng. in power engineering at Sepuluh Nopember Institute of Technology (ITS), Surabaya in 2009. He is mainly research in the microgrid, renewable energy, power system and control. He is currently a Ph.D. candidate at the Department of Electrical Engineering, Institut Teknologi Sepuluh Nopember Surabaya, Indonesia. He can be contacted at email: 7022212006@mhs.its.ac.id.



**Heri Suryatmojo**    received his B.S. degree in electrical engineering from Institut Teknologi Sepuluh Nopember Surabaya, Indonesia in 2004, M.S. degree in electrical engineering from Institut Teknologi Sepuluh Nopember Surabaya, Indonesia in 2006, and Doctor of Engineering from Kumamoto University, Japan in 2010. His current research interests include renewable energy system, converter, distributed power system, power electronics, electric machines and power systems. He is currently a Professor in Institut Teknologi Sepuluh Nopember Surabaya, Indonesia. He can be contacted at email: sryomgt@ee.its.ac.id.



**Feby Agung Pamuji**    received his B.S. degree in electrical engineering from Institut Teknologi Sepuluh Nopember Surabaya, Indonesia in 2009, M.S. degree in electrical engineering from Institut Teknologi Sepuluh Nopember Surabaya, Indonesia in 2012, and Doctor of Engineering from Kumamoto University, Japan in 2018. His current research interests include renewable energy system, converter, power electronics, and electric machines. He is currently a lecturer and researcher in Institut Teknologi Sepuluh Nopember Surabaya, Indonesia. He can be contacted at email: feby@ee.its.ac.id.